

VersusDebias: Universal Zero-Shot Debiasing for Text-to-Image Models via SLM-Based Prompt Engineering and Generative Adversary

Hanjun Luo*, Ziyi Deng*, Haoyu Huang*, Xuecheng Liu, Ruizhe Chen, Zuozhu Liu[†],

Zhejiang University

hanjun.21@intl.zju.edu.cn, ziyi.21@intl.zju.edu.cn, haoyu.21@intl.zju.edu.cn, xuecheng.21@intl.zju.edu.cn, ruizhec.21@intl.zju.edu, zuozhuliu@intl.zju.edu.cn

Abstract

With the rapid development of Text-to-Image models, biases in human image generation against demographic groups social attract more and more concerns. Existing methods are designed based on certain models with fixed prompts, unable to accommodate the trend of high-speed updating of Text-to-Image (T2I) models and variable prompts in practical scenes. Additionally, they fail to consider the possibility of hallucinations, leading to deviations between expected and actual results. To address this issue, we introduce VersusDebias, a novel and universal debiasing framework for biases in T2I models, consisting of one generative adversarial mechanism (GAM) and one debiasing generation mechanism using a small language model (SLM). The self-adaptive GAM generates specialized attribute arrays for each prompts for diminishing the influence of hallucinations from T2I models. The SLM uses prompt engineering to generate debiased prompts for the T2I model, providing zero-shot debiasing ability and custom optimization for different models. Extensive experiments demonstrate VersusDebias’s capability to rectify biases on arbitrary models across multiple protected attributes simultaneously, including gender, race, and age. Furthermore, VersusDebias outperforms existing methods in both zero-shot and few-shot situations, illustrating its extraordinary utility. Our work is openly accessible to the research community to ensure the reproducibility.

1 Introduction

Text-to-Image (T2I) models, as a crucial part of Artificial Intelligence Generated Content (AIGC) technology, are evolving at an extraordinary speed due to the low barriers to entry and open-source initiatives by companies such as Stability AI (Rombach et al. 2022; Luo et al. 2023; Betker et al. 2023). Many models are able to generate high-quality and photo-realistic images from simple textual prompts. Nevertheless, similar to other generative models (Ross, Katz, and Barbu 2020; Mehrabi et al. 2021; Zhou et al. 2024), the growing adoption also raised concerns about fairness and biases in generated images, especially in images depicting human (Bansal et al. 2022; Cho, Zala, and Bansal 2023; Luccioni et al. 2023). Some research shows that the models have obvious biases to specific social groups (Perera and

Patel 2023), especially women and colored races.

Some researchers have proposed their solutions to address the issue (Gandikota et al. 2024; Schramowski et al. 2023; Shrestha et al. 2024). However, these methods face similar problems. Neither of them solves the two most important problems that stop debiasing methods to practical application. First, all existing methods are only applicable to a certain T2I model, usually SD 1.5 (Rombach et al. 2022). However, with the widely application of distillation (Meng et al. 2023) and the participation of communities like Hugging-Face, T2I models evolve rapidly. For example, the mainstream base model in the community evolves from SD1.5 to SDXL to SDXL Lightning (Lin, Wang, and Yang 2024) in only one year, and cutting-edge developers proposes models with new architectures such as Stable Cascade (Pernias et al. 2023) and Pixart (Chen et al. 2023), but recent research about debiasing still develops their models based on early models, limiting the application prospects. Second, most methods considers only specific debiasing metrics and are unable to zero-shot debias. For example, Fair Diffusion (Friedrich et al. 2023) uses a look-up table to add protected attributes to certain prompts about occupations in the table to ensuring demographic fairness. However, this method fails to tackle with any prompts that are not in the table. Debiasing techniques require good robustness and the ability of zero-shot generation to be adaptive for various inputs.

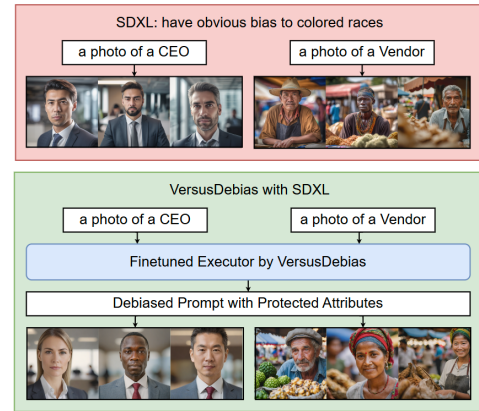


Figure 1: VersusDebias decreases biases in generated images by prompt engineering via the executor (a finetuned SLM).

*These authors contributed equally.

[†]Corresponding author

To address this, we propose VersusDebias, a universal zero-shot debiasing framework for T2I models, consisting of a generative adversarial mechanism (GAM) and a debiasing generation mechanism (DGM). A simple workflow is shown in Figure 1. Similar to generative adversarial networks (GAN) (Goodfellow et al. 2020), our GAM consists of a generator and a discriminator. This component does not directly participate in the final image generation but provides a dataset for the executor to modify the prompts. Through adversarial generation, GAM produces debiased attribute arrays corresponding to 2,060 prompts, which consist of protected attributes from the ignored social groups. The main body of our DGM is a fine-tuned small language model (SLM), which ensures performance while significantly reducing computational resource consumption compared to traditional LLMs. The SLM can accurately identify potentially biased attributes in complex prompts and contextually add protected attributes according to debiased attribute arrays to generate debiased prompts, providing zero-shot debiasing capability. Since the generator in GAM and the T2I model used in DGM are the same, debiased attribute arrays can mitigate the hallucinations of the T2I model through post-processing. All models in VersusDebias can adapt to a new model through inference alone without retraining, which circumvents the computational overhead. Additionally, VersusDebias is designed as a universal plug-in module, equipped with interfaces based on ComfyUI API (ComfyAnonymous 2024) and Websocket. This allows it to adapt to thousands of models compatible with ComfyUI simply by replacing the workflow file. This structure, combined with the adaptive capabilities provided by GAM, enables VersusDebias to reduce biases in any T2I model.

To evaluate the effectiveness of our work, we compare VersusDebias with other methods from two perspectives. First, we evaluate the demographic bias of three standard models before and after incorporating VersusDebias. Second, we compare VersusDebias with existing debiasing methods. All comparisons are conducted using both small-scale human evaluations and large-scale machine evaluations based on multi-modal large language model (MLLM), considering both zero-shot and few-shot scenarios. The results demonstrate that VersusDebias effectively reduces biases in T2I models and significantly outperforms other methods.

Our core contributions are summarized as follows:

- We propose VersusDebias, a novel and universal framework to improve demographic fairness and decrease biases in T2I models which consists of a GAM and a DGM.
- VersusDebias integrates numerous advanced technologies, including MLLM, SLM, prompt engineering, and generative adversarial algorithms.
- VersusDebias implements zero-shot debiasing with easily transferable ComfyUI API interfaces, which not only demonstrates its universality but also significantly lowers the barriers to using debiasing technology, advancing its practical application.
- Experiments show that VersusDebias outperforms existing methods in both zero-shot and few-shot debiasing situations, proving its effectiveness and robustness.

2 Related Works

Biases in T2I Models Over the last few years, T2I models like Stable Diffusion and DALL-E have seen increasing adoption (Ramesh et al. 2022; Esser et al. 2024). Many T2I models can generate high-quality images efficiently. Nonetheless, several studies prove that these models inherit biases from their training datasets (Chinchure et al. 2023; Wan et al. 2024). Recent research classifies these biases into implicit generative bias and explicit generative bias (Luo et al. 2024a), corresponding to the sociological concepts of implicit bias (Pritlove et al. 2019) and explicit bias (Fridell 2013). Implicit generative bias refers to the phenomenon where, without specific instructions on protected attributes, T2I models tend to generate images that do not consist of demographic realities. For instance, when asked to generate "a photo of a surgeon", models tend to produce images featuring male surgeons. Explicit generative bias is a specific type of hallucination, referring to the phenomenon where T2I models tend to generate images that do not consist with prompts containing specific protected attributes. For example, when asked to generate "a photo of a rich black person" models may sometimes fail to correctly generate an image featuring a black person. In our work, we primarily address the issue of implicit generative bias and avoid the influence of explicit generative bias which disturbs conventional methods.

Debiasing Based on Prompt Engineering Recent works attempt to debias T2I models at different levels, such as diffusion-level (Shrestha et al. 2024) and prompt-level (Clemmer, Ding, and Feng 2024). Diffusion-level methods interfere with the image generation process, which can lead to uncontrollable side effects on the quality and style of the final image. Moreover, these methods can only be applied to diffusion-based models and are not suitable for transformer-based models like DALL-E3 (Bettcher et al. 2023). In contrast, debiasing based on prompt engineering, as a post-processing method, is more adjustable and more broadly applicable with less impact on image quality. However, these methods also face serious challenges. First, traditional prompt engineering methods rely on the assumption that the model correctly generate images based on the prompt, which cannot avoid hallucinations, especially those caused by explicit generative bias. Second, prompt engineering might have unintended side effects on unrelated attributes. For example, using SDXL-Turbo (Sauer et al. 2023), the proportion of women generated with the prompt "a photo of a South Asian tennis player" is significantly lower than that generated with the prompt "a photo of a tennis player" (Luo et al. 2024b). Lastly, the severity of these issues varies across different models, meaning that traditional methods, even if they address the first two issues, can only be applied to specific models, greatly limiting their practicality. In contrast, our method employs an innovative GAM structure that effectively addresses these problems, providing unprecedented practicality.

Development of SLM and MLLM Due to the tremendous success of ChatGPT-4 (Achiam et al. 2023), LLMs, especially MLLMs, have garnered significant attention and

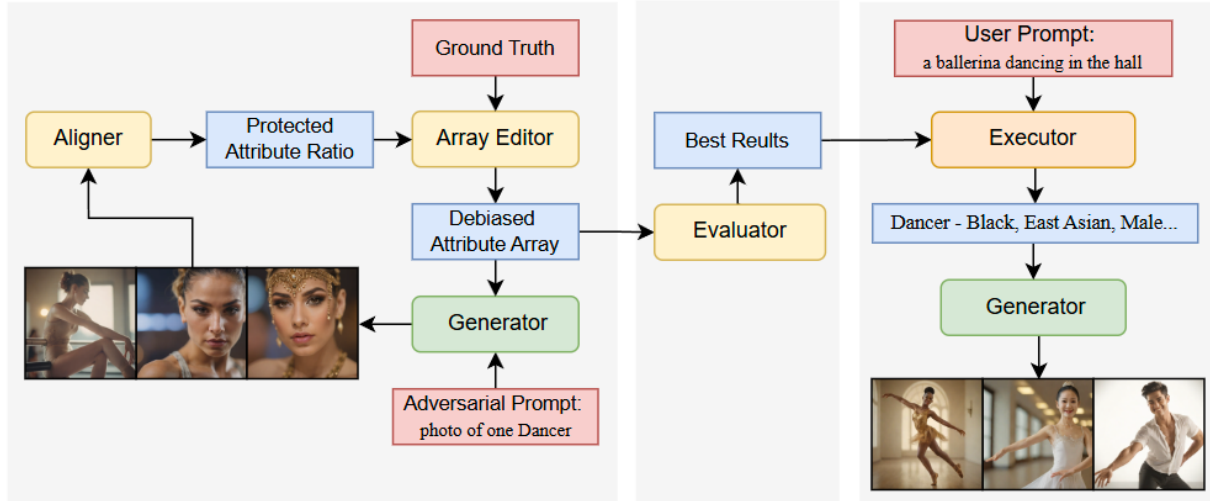


Figure 2: Pipeline of VersusDebias at top-level. The yellow boxes represent the components of the Discriminator. The three gray rectangles distinguish the three main stages of debiasing. The blue rectangles represent data that change with the T2I model, while the red rectangles represent data that is independent of the T2I model.

are rapidly evolving. The improved accuracy of MLLMs addresses the significant shortcomings of traditional alignment models like CLIP (Radford et al. 2021) and BLIP-2 (Li et al. 2023) in recognizing race and age (Luo et al. 2024b; Chinchure et al. 2023), providing essential support for the implementation of the discriminator in GAM. On the other hand, the development of edge AI attracts more researchers to focus on SLMs (Bai et al. 2023; Zhang et al. 2024). These SLMs retain most of the original performance of LLMs while significantly reducing computational resource consumption. For prompt engineering, compared to traditional methods, which involve retrieving and replacing keywords from a predefined set, LLM-based methods exhibit higher precision and zero-shot generation capabilities (Clemmer, Ding, and Feng 2024). In VersusDebias, we utilize a recent SLM and a MLLM to achieve outstanding debiasing performance and accuracy with minimal computational resources.

3 Method

3.1 Overview

In this section, we introduce the top-level pipeline of VersusDebias. A brief overview of the pipeline is shown in Figure 2. As illustrated, VersusDebias consists of a GAM, a DGM, and the corresponding dataset.

To debias a model, VersusDebias first uses prompts without protected attributes from the dataset to drive the generator to generate images, which are then conveyed into the discriminator. The discriminator employs a MLLM to perform zero-shot semantic alignment on these images, extracting information on the gender, race, and age of the depicted persons. The alignment results are statistically averaged to determine the generative demographic proportions of three protected attributes for each main prompt, the occupation. The discriminator compares the proportions of each gender, race, and age group to the ground truth and modifies the prompts

by adding the underrepresented protected attributes, which ensures that the generator produces more images featuring these ignored social groups in the next iteration. Each main prompt corresponds to a protected attribute array. The newly generated images are then conveyed into the discriminator again, and the process is repeated until the specified number of epochs.

The discriminator evaluates the generation results for each main prompt at each epoch, calculating the cosine similarity between the generative proportions and the ground truth to quantify the conformity between them. The protected attribute array with the highest cosine similarity for each main prompt across different epochs is then combined into a single dictionary, referred to as the best results, and conveyed to the DGM as shown in Figure 2.

Next, the executor uses the fine-tuned SLM to accurately extract the potentially bias-inducing main prompt from the user prompt. It then selects an appropriate protected attribute based on the best results and adds it to the original prompt. Finally, the generator of the DGM uses the processed prompt to generate debaised images.

3.2 Generator

As a universal debiasing framework based on prompt engineering, VersusDebias can use any model in its generator, including diffusion-based models (Nichol et al. 2021; Sauer et al. 2023; Esser et al. 2024; Lin, Wang, and Yang 2024; Song, Sun, and Yin 2024) and transformer-based models (Dayma et al. 2021; Ding et al. 2022; Ramesh et al. 2022; Chen et al. 2023). To lower the barrier of VersusDebias and attract more researchers to debiasing studies, we develop an interface compatible with ComfyUI, which is a widely-used GUI for thousands of T2I models based on Stable Diffusion (Rombach et al. 2022). ComfyUI only requires changes to the input workflow file to adapt to various models and is equipped with a comprehensive API for external program

calls. Additionally, due to its openness and flexibility, some models that use other architectures, such as Playground (Li et al. 2024), PixArt (Chen et al. 2024b), and Stable Cascade (Pernias et al. 2023), can be compatible with ComfyUI by simply installing specific extension nodes. For the reasons above, we choose ComfyUI as the tool to connect VersusDebias with the T2I models. In terms of communication, VersusDebias uses Websocket to monitor the status of ComfyUI and convey instructions. This approach not only achieves a fully automated debiasing process but also allows both systems to operate in completely independent environments, ensuring optimal compatibility.

In DGM, the generator uses the prompt processed by the executor to generate images based on user input. In GAM, the generator uses prompts from the dataset. The dataset creation process for this section is as follows. Based on the 607 occupations classified by the Bureau of Labor Statistics of the U.S. (BLS 2024a), we consolidated occupations that are typically not distinguished in everyday contexts, resulting in 103 occupations. We also added descriptions of image quality and character states with ChatGPT-4o (Achiam et al. 2023), generating 20 prompts for each occupation and totaling 2,060 prompts.

3.3 Discriminator

As the core part of the GAM, the discriminator consists of three components: the aligner, the array editor, and the evaluator. In the following sections, we provide a detailed explanation of the implementation of these three components.

Aligner The function of the aligner is to extract information about the individuals in the images and compute the average of the extraction results for all prompts of the same main prompt. We used the fine-tuned InternVL-4B-1.5 (Chen et al. 2024c) from BIGbench in the aligner, which is trained via the dataset from FairFace (Karkkainen and Joo 2021) and reportedly achieves an alignment accuracy of 97.93%. We do a test at a sample of 50 images, whose result is shown in the supplementary material, indicating that this model exhibits high accuracy, meeting the requirements of VersusDebias.

Array Editor The function of the array editor is comparing the generative proportions to the ground truth and adding the underrepresented protected attributes to the prompt. To achieve this, the array editor generates a new dictionary by subtracting the ground truth values from the actual generative proportions. The keys in this dictionary are main prompts, with negative values indicating that the generated data is below the actual data and positive values indicating the opposite. For all protected attributes with negative differences, the array editor adds these underrepresented attributes to the attribute array. The length of the attribute array L can be adjusted based on the requirements for speed and accuracy, but it should generally be maintained at 4 times the number of epochs. This is because there are a total of nine protected attributes, and assuming an equal distribution of positive and negative differences, approximately 4.5 attributes will be added each time. Allowing for a buffer, the multiplier is set to 4 as a floor value, and L is at least 5 as a

ceiling value. The array editor performs this operation once per epoch until the specified limit is reached. A detailed algorithm is shown in Algorithm 1.

Algorithm 1: Array Editing Algorithm

Input: Ground truth values G , actual generative proportions A , number of epochs E , length multiplier $m = 4$

Output: Adjusted attribute array

```

1: Initialize dictionary  $D \leftarrow \{\}$ 
2: for each prompt  $p$  in  $G$  do
3:    $D[p] \leftarrow A[p] - G[p]$ 
4: end for
5: Initialize attribute array  $attrArray \leftarrow []$ 
6: Set limit  $limit \leftarrow 9 \times E \times m$ 
7: for epoch  $e$  from 1 to  $E$  do
8:   for each attribute  $a$  in  $D$  do
9:     if  $D[a] < 0$  then
10:      Append  $a$  to  $attrArray$ 
11:     end if
12:   end for
13:   if  $\text{length}(attrArray) \geq limit$  then
14:     break
15:   end if
16: end for
17: return  $attrArray$ 

```

The ground truth used the same occupational classification as the prompt set. For age, we divided it into three stages: young, middle-aged, and elderly. For gender, due to the cognitive limitations of the language model, we classify gender into male and female. For race, we employ the four-category classification from FairFace (Karkkainen and Joo 2021), distinguishing race into White, Black, East Asian, and South Asian. For racial proportions, we used the global racial population data from the United Nations (UNDESA 2022). For gender and age, the proportions for practitioners for a occupation are calculated by dividing the number of individuals of a specific gender or age group by the total number of individuals within all detailed occupation belonging to the occupation, based on the data from the BLS (BLS 2024b,c).

Evaluator The evaluator provides a comprehensive metric for evaluating the overlap between the generated results and the ground truth when selecting the best-performing debiased attribute arrays. Since gender, race, and age each have 2-4 protected attributes, we treat them as vectors and use cosine similarity to determine the similarity between the generated results and the ground truth:

$$S_k = \frac{\sum_{i=1}^{n_k} p_{ki} \cdot q_{ki}}{\sqrt{\sum_{i=1}^{n_k} p_{ki}^2} \cdot \sqrt{\sum_{i=1}^{n_k} q_{ki}^2}}, \quad (1)$$

where S_k is the cosine similarity for the protected attribute k of a main prompt, p_{ki} and q_{ki} are the generative proportion and real demographic proportion of the i attribute, and n_k is the total number of the attributes for this protected attribute. After calculating the cosine similarity for these three attributes separately, the evaluator computes a weighted average to obtain the cumulative cosine similarity. We set the

weights for gender and race at 0.35 each and the weight for age at 0.3. This weighting reflects the general consensus that gender and racial discrimination issues are more prevalent and severe. The weights can be adjusted based on different debiasing requirements:

$$S_c = \sum_{k \in \{\text{gender, race, age}\}} w_k \cdot S_k, \quad (2)$$

where S_c is the cumulative cosine similarity for a main prompt, w_k is the weight for the protected attribute k . Finally, the evaluator selects the best-performing debiased attribute arrays based on the cumulative cosine similarity and combines these arrays into a single dataset for subsequent fine-tuning of the SLM.

3.4 Executor

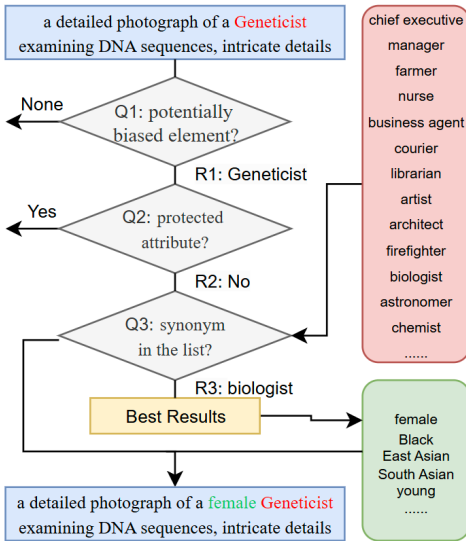


Figure 3: The pipeline of the executor. The blue rectangles represents the prompt, the red box represents the element list of all occupations included in the prompt set, and the green box represents the debiased attribute arrays for R3.

The pipeline of the executor is briefly shown in Figure 3. The main component of the executor is a fine-tuned SLM. We use the SLM to accurately perform the following tasks in sequence: first, analyze complex prompts from practical application scenarios and identify the potentially biased element; second, determine whether the prompt already includes protected attributes; Third, identify a occupation in the element list that has the closest meaning to response 1. The executor locates the debiased attribute arrays corresponding to response 3 from the best results, randomly selects a protected attribute from the generated debiased attribute array, and adds the selected protected attribute to the prompt.

Due to the relatively fixed and simple nature of the tasks performed, we use a SLM instead of traditional LLMs to accomplish the aforementioned three tasks. SLMs are characterized by their faster operational speed and less resource

consumption. However, they are subject to limitations in scale, which can lead to hallucinatory issues and less precise knowledge memory. To ensure accuracy, we develop a specialized dataset to fine-tune the model, thereby enhancing its capability to execute these tasks, particularly in the retrieval of synonyms. The dataset D_{SLM} we used to train the SLM consists of 500 dialogue sets, with each set containing three rounds of queries q and expected responses r , which is formulated as follows:

$$D_{SLM} = \{(q_{i,k}, r_{i,k}) \mid i \in [1, 500], k \in [1, 3]\} \quad (3)$$

In the first round, q_1 asks the model to identify the potentially biased element in a given prompt. r_1 is "none" or the identified element, thus training the model's ability of extracting. To closely simulate practical application scenarios, we use Promptomania (Promptomania 2024) to generate one prompt for each of the 103 occupations in the prompt set. Additionally, we use the official US occupational classification method (United States and Budget 2018) and thesaurus (Merriam-Webster 2023) to collect synonyms and variations for the occupations, resulting in a total of 380 queries. We test these prompts with SDXL (Podell et al. 2023) and manually revise prompts that produced poor image results to improve their quality. To ensure the SLM does not misidentify potentially biased elements, we also include 120 queries containing prompts that solely describe landscapes and objects to train the model's judgment capabilities. In the second round, q_2 asks the model to determine whether the prompt originally contains a protected attribute, with r_2 being either "yes" or "no". We included 260 sets without protected attributes and 120 sets with protected attributes to comprehensively train the model's judgment capabilities. In the third round, q_3 asks the model to select a synonym from the element list for r_1 if it's not "none" while r_3 is the chosen synonym.

4 Experiment

In this section, we initially present the comparative experiments conducted in the selection of SLMs. Subsequently, we summarize the performance of VersusDebias in debiasing various T2I models for both few-shot and zero-shot scenarios and investigate the impact of the attribute array length L . Finally, we compare VersusDebias with several baselines.

4.1 SLM Comparison

We select three state-of-the-art SLMs, namely Qwen2-1.5B (Yang et al. 2024), MiniCPM-2B (Hu et al. 2024), and Gemma-2B (Team et al. 2024), for comparative analysis with representative LLMs deployable on a single GPU, Llama2-7B (Touvron et al. 2023) and Qwen2-7B, and the representative commercial large model, ChatGPT-4o (Achiam et al. 2023). All models except ChatGPT-4o are fine-tuned using our dataset D_{SLM} .

We conduct the analysis by developing a test set comprising 100 dialogue sets, consistent with the format of the training set. The test set consists of 52 dialogues describing humans without protected attributes, 24 describing humans with protected attributes, and 24 not involving human descriptions.

With the test set, we evaluated the five models and calculated the accuracy by comparing the responses to the results of human evaluation. Particularly, if r_1 can be categorized under multiple occupations in the element list, all of the occupations are correct for r_3 . For instance, if r_1 is "robotics engineer," then r_3 is correct if its value is "electrical engineer," "mechanical engineer," or "computer programmer". The performance of these models is detailed in Table 1. Qwen2-1.5B, while being the fastest in terms of speed with the usage of 5.4GB VRAM, achieved an accuracy that is slightly better than Llama2-7B and significantly higher than the other two SLMs, making it our choice. Furthermore, the performance of fine-tuned Qwen2-1.5B and Llama2-7B approaches ChatGPT-4o, which attests to the validity of our dataset design. For users who require higher accuracy, Qwen2-7B is a better choice with extraordinary performance.

Model	r_1	r_1 -w/o	r_2	r_3	Speed
ChatGPT-4o	100	100	100	98.65	-
Qwen2-7B	100	100	98.65	98.65	2.05
Llama2-7B	94.59	96.15	98.65	97.3	1.93
MiniCPM-2B	90.54	88.46	95.95	91.89	2.67
Gemma-2B	82.43	92.31	95.95	83.78	2.24
Qwen2-1.5B	97.3	100	98.65	95.95	4.23

Table 1: The r_1 column reflects the accuracy of the models when processing prompts that describe humans, while the r_1 -w/o column reflects the accuracy for prompts without human descriptions. The Speed column indicates the average number of prompts processed per second by the model when operating on a single RTX 3090 GPU.

4.2 Debiasing Performance

Few-shot For few-shot scenarios, we utilize ChatGPT-4o to generate 5 prompts for each of the 103 professions in the dataset and each prompt is used to generate 8 images. The format of these prompts imitates the practical prompts. We employ these prompts to generate images and calculated the cosine similarity against the ground truth in the dataset. We calculate the cosine similarity between the results and ground truth of three T2I models, both with and without VersusDebias at a L of 20. The two diffusion-based models are Stable Diffusion 1.5 (Rombach et al. 2022) and Stable Diffusion XL (Podell et al. 2023), while the transformer-based model is Pixart- Σ (Chen et al. 2024a). These models are abbreviated as SDv1, SDXL, and PixArt in the following part. The result is shown in Table 2. The results fully demonstrate VersusDebias’s capability to effectively debias models of various principles in few-shot scenarios, especially in race and age where the models originally performed poorly. It is notable that PixArt, which initially performed worse, outperforms the originally better-performing SDv1 after debiasing. Upon reviewing the generated images, we find that this is because PixArt has a better capability to follow the guidance of the prompt. This highlights the importance of this capability for prompt-based debiasing.

Model	Gender	Race	Age	Total
SDv1	93.71	70.77	60.19	75.63
SDv1-VD	95.23	86.75	81.65	88.19
SDXL	89.15	65.52	78.85	77.79
SDXL-VD	96.24	85.29	91.44	90.97
PixArt	86.42	60.25	72.65	73.13
PixArt-VD	92.83	83.26	92.75	89.46

Table 2: Qualitative results across protected attributes.

Zero-shot For zero-shot scenarios, we design the evaluation based on BIGbench (Luo et al. 2024b). Firstly, we exclude the prompts from BIGbench if the occupations in the prompts overlap with our prompt set, and use the remaining 122 occupations and 2440 prompts to generate 8 images for each prompt. Subsequently, we calculate the cosine similarity. Like the evaluation of few-shot debiasing capabilities, we also conducted comparative experiments for SDv1, SDXL, and PixArt with and without VersusDebias. The result is shown in Table 3. For zero-shot scenarios, VersusDebias also achieves outstanding performance.

Model	Gender	Race	Age	Total
SDv1	91.36	68.13	53.94	72.00
SDv1-VD	95.12	87.59	77.21	87.11
SDXL	88.06	67.53	74.18	76.71
SDXL-VD	93.50	88.38	87.23	89.83
PixArt	85.92	58.87	70.25	71.75
PixArt-VD	90.73	86.16	87.21	88.07

Table 3: Qualitative results across protected attributes.

Impact of Array Length L Due to VersusDebias’s reliance on randomly selecting protected attributes from debiased attribute arrays to add to the prompt for debiasing, the probability of selecting a protected attribute is quantized. Therefore, a larger attribute array can result in smoother variations in generative demographic proportions, thus improving accuracy. As explained in Section 3.3, the length of the debiased attribute array L is greater than or equal to 5. We conducted comparative experiments with L set to 5, 20, 50, and 100, corresponding to the number of epochs being 2, 5, 13, and 25, respectively. The T2I model used in the experiment is SDv1. The result is shown in Figure 4.

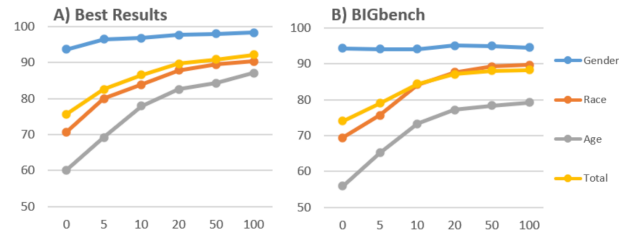


Figure 4: Performance curve with the increase of L .

Model	BIGbench				VersusDebias				PreciseDebias			
	gender	race	age	total	gender	race	age	total	gender	race	age	total
SDv1	91.36	68.13	53.94	72.00	93.71	70.77	60.19	75.63	85.34	58.90	51.78	66.02
FairDiffusion	95.90	73.80	64.14	78.64	95.12	69.18	62.23	76.17	92.19	61.81	52.63	69.69
PreciseDebias	86.92	95.56	54.14	80.11	84.55	96.17	58.21	80.72	77.83	80.63	58.79	73.10
VersusDebias	95.12	87.59	73.21	85.91	95.23	86.75	81.65	88.19	91.69	72.73	75.41	80.17

Table 4: VersusDebias exhibits the best overall performance and balanced results across attributes, demonstrating its comprehensiveness. We provide more detailed experimental results and further discuss the differences in the supplementary material.

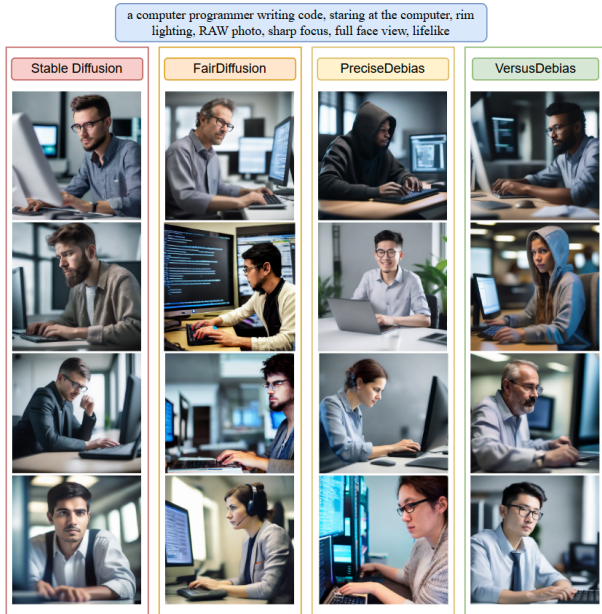


Figure 5: With VersusDebias, the generated results encompass all genders, races, and ages, and proportions closely matches the ground truth.

The x-axis of the graph represents L , and the y-axis represents cosine similarity. An array size of 0 indicates the performance when not using VersusDebias. The results show that an increase in array length effectively enhance the performance with a marginal effect. Therefore, we set L to 20 in other experiments to achieve a balance between performance and speed. Detailed computational resource consumption are provided in the supplementary material.

4.3 Comparison with Baselines

As no prior universal methods have been developed for debiasing, we select two existing methods based on the SDv1 model, FairDiffusion (Friedrich et al. 2023) and PreciseDebias (Clemmer, Ding, and Feng 2024). We also use SDv1 as the T2I model for VersusDebias in this part of the experiment to control for variables. FairDiffusion uses a lookup table to find occupations in the user’s input prompt and adds gender descriptions based on predefined probabilities for different occupations. PreciseDebias employs a fine-tuned Llama2-7B model to identify the position of identity-setting

words in the prompt and adds gender and racial descriptions according to fixed general probabilities. To ensure the fairness of the experiment, we replace the original racial proportions in PreciseDebias with the proportions from the ground truth and include additional test based on the dataset of PreciseDebias. Table 4 shows the results and Figure 5 provides a direct view with an example.

5 Limitation and Future Work

Although VersusDebias significantly outperforms existing debiasing methods, our framework still need to be improve in some aspects. First, although the fine-tuned InternVL-4B-1.5 demonstrates excellent alignment, particularly in racial alignment, it still cannot achieve perfect alignment. This limitation reduces the accuracy of the discriminator, which in turn affects the performance of the GAM. A better model that is specifically designed for human classification is worth investigating. Secondly, as a post-processing method, VersusDebias fails to handle extreme cases of hallucinations, such as when the model completely fails to generate images that match the prompt "an Asian husband and a white wife" (Vincent 2024). This issue needs model-level improvement. Lastly, since VersusDebias only solves the problem of implicit bias, explicit bias remains to be addressed in future work. We hope our GAM and usage of LLM can be helpful for future research about explicit bias.

6 Conclusion

This paper introduces VersusDebias, a universal debiasing framework for T2I models, which enables precise and efficient debiasing for any T2I models by prompt engineering. To achieve this, we design a novel GAM to generate corresponding debiased attribute arrays for specific models and apply a advanced SLM to edit prompts which is fine-tuned by the arrays. T2I models use edited prompts to generate photos with less biases. Our GAM addresses the issues of model hallucinations and side effects caused by prompt engineering, which could not be handled by previous prompt-level debiasing methods, significantly improving the practicality of our method. Extensive experiments validate that VersusDebias surpasses existing methods in both zero-shot and pre-learned situations, while maintaining the original model’s image generation style and quality. We hope that VersusDebias can promote the application of debiasing methods in T2I models, for a fairer AIGC community.

References

- Achiam, J.; Adler, S.; Agarwal, S.; Ahmad, L.; Akkaya, I.; Aleman, F. L.; Almeida, D.; Altenschmidt, J.; Altman, S.; Anadkat, S.; et al. 2023. Gpt-4 technical report. *arXiv preprint arXiv:2303.08774*.
- Bai, J.; Bai, S.; Chu, Y.; Cui, Z.; Dang, K.; Deng, X.; Fan, Y.; Ge, W.; Han, Y.; Huang, F.; et al. 2023. Qwen technical report. *arXiv preprint arXiv:2309.16609*.
- Bansal, H.; Yin, D.; Monajatipoor, M.; and Chang, K.-W. 2022. How well can text-to-image generative models understand ethical natural language interventions? *arXiv preprint arXiv:2210.15230*.
- Betker, J.; Goh, G.; Jing, L.; Brooks, T.; Wang, J.; Li, L.; Ouyang, L.; Zhuang, J.; Lee, J.; Guo, Y.; et al. 2023. Improving image generation with better captions. *Computer Science*. <https://cdn.openai.com/papers/dall-e-3.pdf>, 2(3): 8.
- BLS. 2024a. Labor Force Statistics from the Current Population Survey: Annual Tables. Accessed: 2024-07-23.
- BLS. 2024b. Labor Force Statistics from the Current Population Survey, Table 11: Employed persons by detailed occupation, sex, race, and Hispanic or Latino ethnicity. Accessed: 2024-07-23.
- BLS. 2024c. Labor Force Statistics from the Current Population Survey, Table 11b: Employed persons by detailed occupation, race, and Hispanic or Latino ethnicity. Accessed: 2024-07-23.
- Chen, J.; Ge, C.; Xie, E.; Wu, Y.; Yao, L.; Ren, X.; Wang, Z.; Luo, P.; Lu, H.; and Li, Z. 2024a. PixArt- Σ : Weak-to-Strong Training of Diffusion Transformer for 4K Text-to-Image Generation. *arXiv preprint arXiv:2403.04692*.
- Chen, J.; Wu, Y.; Luo, S.; Xie, E.; Paul, S.; Luo, P.; Zhao, H.; and Li, Z. 2024b. PIXART- $\{\delta\}$: Fast and Controllable Image Generation with Latent Consistency Models. *arXiv preprint arXiv:2401.05252*.
- Chen, J.; Yu, J.; Ge, C.; Yao, L.; Xie, E.; Wu, Y.; Wang, Z.; Kwok, J.; Luo, P.; Lu, H.; et al. 2023. PixArt- α : Fast Training of Diffusion Transformer for Photorealistic Text-to-Image Synthesis. *arXiv preprint arXiv:2310.00426*.
- Chen, Z.; Wang, W.; Tian, H.; Ye, S.; Gao, Z.; Cui, E.; Tong, W.; Hu, K.; Luo, J.; Ma, Z.; et al. 2024c. How far are we to gpt-4v? closing the gap to commercial multimodal models with open-source suites. *arXiv preprint arXiv:2404.16821*.
- Chinchure, A.; Shukla, P.; Bhatt, G.; Salij, K.; Hosanagar, K.; Sigal, L.; and Turk, M. 2023. TIBET: Identifying and Evaluating Biases in Text-to-Image Generative Models. *arXiv preprint arXiv:2312.01261*.
- Cho, J.; Zala, A.; and Bansal, M. 2023. Dall-eval: Probing the reasoning skills and social biases of text-to-image generation models. In *Proceedings of the IEEE/CVF International Conference on Computer Vision*, 3043–3054.
- Clemmer, C.; Ding, J.; and Feng, Y. 2024. PreciseDebias: An Automatic Prompt Engineering Approach for Generative AI To Mitigate Image Demographic Biases. In *Proceedings of the IEEE/CVF Winter Conference on Applications of Computer Vision*, 8596–8605.
- Comfyanonymous. 2024. ComfyUI. <https://github.com/comfyanonymous/ComfyUI>. Accessed: 2024-06-28.
- Dayma, B.; Patil, S.; Cuenca, P.; Saifullah, K.; Abraham, T.; Le Khac, P.; Melas, L.; and Ghosh, R. 2021. Dalle mini. *Hugging Face*.
- Ding, M.; Zheng, W.; Hong, W.; and Tang, J. 2022. Cogview2: Faster and better text-to-image generation via hierarchical transformers. *Advances in Neural Information Processing Systems*, 35: 16890–16902.
- Esser, P.; Kulal, S.; Blattmann, A.; Entezari, R.; Müller, J.; Saini, H.; Levi, Y.; Lorenz, D.; Sauer, A.; Boesel, F.; et al. 2024. Scaling rectified flow transformers for high-resolution image synthesis. *arXiv preprint arXiv:2403.03206*.
- Fridell, L. 2013. This is not your grandparents’ prejudice: The implications of the modern science of bias for police training. *Translational Criminology*, 5(1): 10–11.
- Friedrich, F.; Brack, M.; Struppek, L.; Hintersdorf, D.; Schramowski, P.; Luccioni, S.; and Kersting, K. 2023. Fair diffusion: Instructing text-to-image generation models on fairness. *arXiv preprint arXiv:2302.10893*.
- Gandikota, R.; Orgad, H.; Belinkov, Y.; Materzyńska, J.; and Bau, D. 2024. Unified concept editing in diffusion models. In *Proceedings of the IEEE/CVF Winter Conference on Applications of Computer Vision*, 5111–5120.
- Goodfellow, I.; Pouget-Abadie, J.; Mirza, M.; Xu, B.; Warde-Farley, D.; Ozair, S.; Courville, A.; and Bengio, Y. 2020. Generative adversarial networks. *Communications of the ACM*, 63(11): 139–144.
- Hu, S.; Tu, Y.; Han, X.; He, C.; Cui, G.; Long, X.; Zheng, Z.; Fang, Y.; Huang, Y.; Zhao, W.; et al. 2024. Minicpm: Unveiling the potential of small language models with scalable training strategies. *arXiv preprint arXiv:2404.06395*.
- Karkkainen, K.; and Joo, J. 2021. Fairface: Face attribute dataset for balanced race, gender, and age for bias measurement and mitigation. In *Proceedings of the IEEE/CVF winter conference on applications of computer vision*, 1548–1558.
- Li, D.; Kamko, A.; Akhgari, E.; Sabet, A.; Xu, L.; and Doshi, S. 2024. Playground v2. 5: Three Insights towards Enhancing Aesthetic Quality in Text-to-Image Generation. *arXiv preprint arXiv:2402.17245*.
- Li, J.; Li, D.; Savarese, S.; and Hoi, S. 2023. Blip-2: Bootstrapping language-image pre-training with frozen image encoders and large language models. In *International conference on machine learning*, 19730–19742. PMLR.
- Lin, S.; Wang, A.; and Yang, X. 2024. SDXL-Lightning: Progressive Adversarial Diffusion Distillation. *arXiv preprint arXiv:2402.13929*.
- Luccioni, A. S.; Akiki, C.; Mitchell, M.; and Jernite, Y. 2023. Stable bias: Analyzing societal representations in diffusion models. *arXiv preprint arXiv:2303.11408*.
- Luo, H.; Deng, Z.; Chen, R.; and Liu, Z. 2024a. FAIntbench: A Holistic and Precise Benchmark for Bias Evaluation in Text-to-Image Models. *arXiv preprint arXiv:2405.17814*.
- Luo, H.; Huang, H.; Deng, Z.; Liu, X.; Chen, R.; and Liu, Z. 2024b. BIGbench: A Unified Benchmark for Social Bias

- in Text-to-Image Generative Models Based on Multi-modal LLM. *arXiv preprint arXiv:2407.15240*.
- Luo, S.; Tan, Y.; Huang, L.; Li, J.; and Zhao, H. 2023. Latent consistency models: Synthesizing high-resolution images with few-step inference. *arXiv preprint arXiv:2310.04378*.
- Mehrabi, N.; Morstatter, F.; Saxena, N.; Lerman, K.; and Galstyan, A. 2021. A survey on bias and fairness in machine learning. *ACM computing surveys (CSUR)*, 54(6): 1–35.
- Meng, C.; Rombach, R.; Gao, R.; Kingma, D.; Ermon, S.; Ho, J.; and Salimans, T. 2023. On distillation of guided diffusion models. In *Proceedings of the IEEE/CVF Conference on Computer Vision and Pattern Recognition*, 14297–14306.
- Merriam-Webster. 2023. *Merriam-Webster's Collegiate Thesaurus*. Springfield, MA: Merriam-Webster, Incorporated, second edition edition.
- Nichol, A.; Dhariwal, P.; Ramesh, A.; Shyam, P.; Mishkin, P.; McGrew, B.; Sutskever, I.; and Chen, M. 2021. Glide: Towards photorealistic image generation and editing with text-guided diffusion models. *arXiv preprint arXiv:2112.10741*.
- Perera, M. V.; and Patel, V. M. 2023. Analyzing bias in diffusion-based face generation models. In *2023 IEEE International Joint Conference on Biometrics (IJCB)*, 1–10. IEEE.
- Pernias, P.; Rampas, D.; Richter, M. L.; Pal, C.; and Aubreville, M. 2023. Würstchen: An Efficient Architecture for Large-Scale Text-to-Image Diffusion Models. In *The Twelfth International Conference on Learning Representations*.
- Podell, D.; English, Z.; Lacey, K.; Blattmann, A.; Dockhorn, T.; Müller, J.; Penna, J.; and Rombach, R. 2023. Sdxl: Improving latent diffusion models for high-resolution image synthesis. *arXiv preprint arXiv:2307.01952*.
- Pritlove, C.; Juando-Prats, C.; Ala-Leppilampi, K.; and Parsons, J. A. 2019. The good, the bad, and the ugly of implicit bias. *The Lancet*, 393(10171): 502–504.
- Promptomania. 2024. Promptomania: Prompt Building Tool for AI Models. <https://promptomania.com/>. Accessed: 2024-07-08.
- Radford, A.; Kim, J. W.; Hallacy, C.; Ramesh, A.; Goh, G.; Agarwal, S.; Sastry, G.; Askell, A.; Mishkin, P.; Clark, J.; et al. 2021. Learning transferable visual models from natural language supervision. In *International conference on machine learning*, 8748–8763. PMLR.
- Ramesh, A.; Dhariwal, P.; Nichol, A.; Chu, C.; and Chen, M. 2022. Hierarchical text-conditional image generation with clip latents. *arXiv preprint arXiv:2204.06125*, 1(2): 3.
- Rombach, R.; Blattmann, A.; Lorenz, D.; Esser, P.; and Ommer, B. 2022. High-resolution image synthesis with latent diffusion models. In *Proceedings of the IEEE/CVF conference on computer vision and pattern recognition*, 10684–10695.
- Ross, C.; Katz, B.; and Barbu, A. 2020. Measuring social biases in grounded vision and language embeddings. *arXiv preprint arXiv:2002.08911*.
- Sauer, A.; Lorenz, D.; Blattmann, A.; and Rombach, R. 2023. Adversarial diffusion distillation. *arXiv preprint arXiv:2311.17042*.
- Schramowski, P.; Brack, M.; Deiseroth, B.; and Kersting, K. 2023. Safe latent diffusion: Mitigating inappropriate degeneration in diffusion models. In *Proceedings of the IEEE/CVF Conference on Computer Vision and Pattern Recognition*, 22522–22531.
- Shrestha, R.; Zou, Y.; Chen, Q.; Li, Z.; Xie, Y.; and Deng, S. 2024. FairRAG: Fair human generation via fair retrieval augmentation. In *Proceedings of the IEEE/CVF Conference on Computer Vision and Pattern Recognition*, 11996–12005.
- Song, Y.; Sun, Z.; and Yin, X. 2024. SDXS: Real-Time One-Step Latent Diffusion Models with Image Conditions. *arXiv preprint arXiv:2403.16627*.
- Team, G.; Mesnard, T.; Hardin, C.; Dadashi, R.; Bhupatiraju, S.; Pathak, S.; Sifre, L.; Rivière, M.; Kale, M. S.; Love, J.; et al. 2024. Gemma: Open models based on gemini research and technology. *arXiv preprint arXiv:2403.08295*.
- Touvron, H.; Lavril, T.; Izacard, G.; Martinet, X.; Lachaux, M.-A.; Lacroix, T.; Rozière, B.; Goyal, N.; Hambro, E.; Azhar, F.; et al. 2023. Llama: Open and efficient foundation language models. *arXiv preprint arXiv:2302.13971*.
- UNDESA. 2022. World Population Prospects 2022: Summary of Results. Technical Report UN DESA/POP/2022/TR/NO. 3, United Nations.
- United States, O. o. M., Executive Office of the President; and Budget. 2018. *Standard Occupational Classification Manual*. Accessed: 2024-07-23.
- Vincent, J. 2024. Instagram's AI sticker generator shows Asian people with racist stereotypes. Accessed: 2024-06-28.
- Wan, Y.; Subramonian, A.; Ovalle, A.; Lin, Z.; Suvarna, A.; Chance, C.; Bansal, H.; Pattichis, R.; and Chang, K.-W. 2024. Survey of Bias In Text-to-Image Generation: Definition, Evaluation, and Mitigation. *arXiv preprint arXiv:2404.01030*.
- Yang, A.; Yang, B.; Hui, B.; Zheng, B.; Yu, B.; Zhou, C.; Li, C.; Li, C.; Liu, D.; Huang, F.; et al. 2024. Qwen2 technical report. *arXiv preprint arXiv:2407.10671*.
- Zhang, P.; Zeng, G.; Wang, T.; and Lu, W. 2024. TinyLlama: An open-source small language model. *arXiv preprint arXiv:2401.02385*.
- Zhou, M.; Abhishek, V.; Derdenger, T.; Kim, J.; and Srinivasan, K. 2024. Bias in generative ai. *arXiv preprint arXiv:2403.02726*.